Global Change Biology

Supporting Information

Embracing fine-root system complexity in terrestrial ecosystem modelling

Bin Wang[1*], M. Luke McCormack [2], Daniel M. Ricciuto[1], Xiaojuan Yang[1], and Colleen M. Iversen[1]

1 Environmental Sciences Division, Oak Ridge National Laboratory, Oak Ridge, Tennessee 37830 USA

2 Center for Tree Science, The Morton Arboretum, Lisle, Illinois 60532 USA

* Correspondence: Bin Wang (wangb@ornl.gov or wbwenwu@gmail.com)

1 Realization of TAM

sELM is a simplified version of the Energy Exascale Earth System Model (E3SM) Land Model ELM, a state-of-the-art land surface model developed by Department of Energy, United States (Golaz et al. 2019; Burrows et al. 2020). ELM is traced back to the original CLM4.5 (Oleson et al. 2013**)** and the later version E3SM Land Model (ELM). sELM simplifies ELM by keeping only essential components simulating natural ecosystems in North America including vegetation and soil biogeochemistry (Lu and Ricciuto 2019). Following the same global PFT classification scheme as ELM, vegetation has the same structural pools (with a single fine-root pool) as ELM using the big-leaf approach. Although photosynthesis and GPP are replaced by a neural network

surrogate built from ELM simulations, the whole scheme of allocation of photosynthates remains the same. Soil system, except for the lack of hydrology, is the same as the ELM with a 10-layer profile of 3.8018 m deep. Litter and soil organic matter decomposition follow the CTC (Converging Trophic Cascade) framework (Oleson et al. 2013; Burrows et al. 2020). Plant-microbe competition for mineral nitrogen is achieved via the relative demand approach without further differentiating between nitrogen forms (i.e., NH_4 and NO_3). Such a simplified model, in a more formal sense, is a high-fidelity mechanistic surrogate; by omitting irrelevant processes but keeping all essential components, it eases modifications of structures and processes and reduces computational burden for analyses of uncertainty and sensitivity, contributing to an acceleration of the development-evaluation-application cycle for Earth System Models in particular. Changes introduced to realize TAM are described below in detail following the PPD(Partitioning-Phenology-Distribution) framework.

1.1 Partitioning

We directly introduce three parameters (***frootpar_i***, where *i* indexes the three fine root pools of T, A, and M) to determine the spreading of allocation to a fine-root system (from either photosynthates or storage) among TAM pools. This approach simplifies the partitioning without considering explicitly the processes of movement of carbohydrates across the branching structure. With known partitioning (***frootpar_i***) and fine root C/N (***frootcn_i***), allocation allometry (ratio of allocation to total new growth to allocation to new leaf, *Callom/Nallom*) can be determined following:

$$\begin{cases} Callom = (1+g1)[1+a1+a3(1+a2)] \\ Nallom = \frac{1}{CN_{leaf}} + a_1 \sum_{i=1}^{3} \frac{frootpar\_i}{frootcn\_i} + \frac{a3a4(1+a2)}{CN_{livewood}} + \frac{a3(1-a4)(1+a2)}{CN_{deadwood}} \end{cases} \quad (1)$$

where ***a1*** through ***a4*** are allometric parameters that relate allocation between various tissue types, among which ***a1*** is the ratio of new fine root to new leaf carbon allocation (i.e., ***froot_leaf***), ***a2*** ratio of new coarse root to new stem carbon allocation, ***a3*** ratio of new stem to new leaf carbon allocation, ***a4*** ratio new live wood to new total wood allocation, and ***g1*** allocation ratio of growth respiration carbon to new growth carbon, as well as C/N of both live wood and dead wood. TAM pools are parameterized with different C/N ratios based on consistent observations of descending C/N while fine-root systems branching out (e.g., Pregitzer et al. 1997; McCormack et al. 2015).

1.2 Phenology

In ELM, fine-root production is temporally controlled by leaf phenology in moving carbon from two direct sources: recent photosynthate and storage, making leaf and root production perfectly synchronous. These two sources, though ultimately originating from photosynthesis, can also be referred to as direct and indirect allocation, respectively. The allocation from leaf photosynthates to the fine-root system is based on an allometric relationship between leaves and fine roots (***froot_leaf*** = 1). This allocation is divided between direct allocation to the currently displayed fine-root system (***fcur***) and a storage pool to supply future growth for the whole fine-root system (i.e., indirect allocation; 1 - ***fcur***). This storage-based indirect allocation is also controlled by leaf phenology. Such a totally synchronous treatment between leaf and fine-root production is the case across all current ecosystem models, which, however, does not reflect the increasingly rich evidence that shoot and root phenology are not synchronous (e.g., Perry 1971; Steinaker and Wilson 2008; Steinaker et al. 2010; McCormack et al. 2015b; Abramoff & Finzi

2015; Radville et al. 2016). We make the following 3-step changes to decouple the phenological control of shoot and TAM in both deciduous and evergreen systems.

First, we make evergreen PFTs have the two-source structure of storage and recent photosynthate. In the current ELM, this two-source structure only applies to deciduous PFTs. Evergreen PFTs do not accumulate carbon and nitrogen in the storage pools for fine-root systems; instead, root production is solely determined by direct allocation of new photosynthates (i.e., ***fcur* = 1**), an assumption that lacks empirical support (e.g., Huang et al. 2021). Therefore, this treatment is changed for evergreen PFTs to have the same two-source structure as deciduous PFTs. This structure enables storage-based production of (or indirect allocation to) fine-root systems controlled by TAM phenology.

Then, we decouple TAM phenology from leaf phenology for both deciduous and evergreen PFTs (**Fig.1**). In the current ELM, storage-based initiation of fine roots is synchronous with leaf-based control of unfolding (triggered by a growing degree threshold) and shedding (triggered by a critical day length). This synchronous treatment is changed to allow TAM initiation to behave independently in both deciduous and evergreen systems, which are determined by ***GDDsum*** (growing degree days with a 0-degree base) relative to a threshold value, ***GDDfroot_sum_crit***:

$$GDD_{froot\_sum\_crit} = GDD_{leaf\_sum\_crit} + \Delta GDD_{froot\_leaf} \quad (2)$$

where $\boldsymbol{\Delta GDD_{leaf\_froot}}$ is the difference between leaf and fine root threshold of GDD. Once $\boldsymbol{GDDsum > GDD_{froot\_sum\_crit}}$, TAM initiation is triggered, and fluxes of carbon and nitrogen begin to move from storage pools (CS_{froot_stor}) to the fine-root system. This occurs via transfer pools ($CF_{froot\_stor,froot\_xfer}$) calculated following:

$$CF_{froot\_stor,froot\_xfer} = f_{stor,xfer} CS_{froot\_stor} \quad (3)$$

where $f_{stor,xfer}$ = 0.5, the fraction of current storage pool moved into the transfer pool for display over the incipient onset period (Oleson et al. 2013).

Finally, we make TAM turnover of deciduous PFTs dependent on pool-specific mortality. For deciduous PFTs in the current ELM, the shedding of fine roots is synchronous with leaf shedding, which lacks empirical support. This synchronous treatment is thus changed to allow deciduous fine-root mortality to behave independently in deciduous systems in the same way as the fine roots of evergreen PFTs. See **Section 2.4** on TAM mortality.

1.3 Distribution

In ELM and other land surface models, the prevailing option assumes that fine roots and coarse roots follow the same distribution as determined by prescribed fixed rooting and soil depths following:

$$r_{croot\_i} = \begin{cases} 0.5\left[\exp\left(-r_a z_{h,i-1}\right) + \exp\left(-r_b z_{h,i-1}\right) - \exp\left(-r_a z_{h,i}\right) - \exp\left(-r_b z_{h,i}\right)\right], & for\ 1 \le i < N_{levsoi} \\ 0.5\left[\exp\left(-r_a z_{h,i-1}\right) + \exp\left(-r_b z_{h,i-1}\right)\right], & for\ i = N_{levsoi} \end{cases} \quad (4)$$

where ***ra*** and ***rb*** are PFT-dependent root distribution parameters. Because of the dynamic nature of fine-root systems, the vertical profile is modelled dynamically by assuming horizontal

114 homogenization of TAM (that is, the same distribution profile across T, A, and M) constrained by
115 nutrient and water availability:
116
117 $$r_{froot\_i} = \frac{r_{croot\_i} f_{n\_i} f_{m\_i}}{\sum_{i=1}^{nlevsoi} r_{croot\_i} f_{n\_i} f_{m\_i}} \quad (5)$$
118
119 where ***fn_i*** and ***fm_i*** are the relative availability of nutrients and the relative availability of water
120 at soil layer i, respectively, which are calculated by dividing nutrient or water availability in each
121 layer by the total amount across the whole soil profile. This nutrient constraint means that relatively
122 more of the allocation goes to the depth where the relative nutrient availability is high; that is, a
123 plant can direct allocation and distribution to the place where the nutrients are relatively richer.
124 Note that root-water interactions are beyond the scope of this study and are not included in the
125 analysis below. Such a realization of a dynamic profile contingent on a fixed coarse root profile
126 partly accounts for the notion that coarser roots provide a structural constraint for potential fine-
127 root system distribution dictated by the hierarchical branching structure of root systems.
128
129 **1.4 Mortality and litter input**
130 With a 3-pool structure, turnover of the fine-root system is modelled explicitly in a
131 vertically resolved way by introducing a mortality term. Mortality of fine roots and mycorrhizal
132 fungi is endogenously controlled but subject to exogenous influences (e.g., Eissenstat & Yanai
133 1997; Hendrick and Pregitzer 1997). Therefore, consistent with the current approach in ELM
134 modelling turnover using a mortality parameter in general, TAM mortality in each time step is
135 determined by longevity distinguished among T, A, and M (***froot_long***) and constrained by a
136 depth-correction term (α) as follows:

$$\begin{cases} Mr_{i,j} = \frac{1}{froot\_long\_i}\,\alpha_j \\ \alpha_j = e^{-\frac{dzj}{mort\_depth\_efolding}} \end{cases} \quad (6)$$

where ***froot_long_i*** is longevity of the three TAM pools near the soil surface, ***mort_depth_efolding*** is a constant of mortality rate decrease with depth, and ***dzj*** is depth of soil layer *j*.

Mortality of the T, A, and M pools are parameterized with different but decreasing lifespans based on relatively easy-to-make observations in shallow soil depths (**Table S1**). This pattern is based on field observations of a dramatic increase in survivorship with diameter even within a very narrow range (e.g., ≤ 0.5 mm) (e.g., Reid et al., 1993; Hendrick & Pregitzer 1993; Tierney & Fahey 2002; Edwards et al. 2004; Joslin et al. 2006; Espeleta et al. 2009; Riley et al. 2009; Xia et al. 2010) and direct observations of lifespan and turnover in fungal tissues (Allen and Kitajima 2013; McCormack et al. 2010). The depth-correction term (***α***) further corrects the fine root and fungi longevity (***froot_long***) for increasing lifespan with soil depth (e.g., Baddeley and Waston 2005; Iversen et al. 2008; McCormack et al. 2012; Germon et al 2015; Gu et al. 2017). This depth-based correction partly accounts for the plasticity of fine-root systems in response to vertical variability in soil resource availability (e.g., Pregitzer et al. 1993; Eissenstat and Yanai, 1997).

An explicit turnover of fine-root systems means explicit production of litters from the three pools. The TAM structure is coupled with existing litter decomposition model simply by aggregating litters across the 3 pools and depositing them in the three vertically resolved soil litter pools—labile, cellulose/hemicellulose, and lignin (Oleson et al. 2013). Each of the three fine-root

pools is parameterized with fractions of these three different groups in terms of C (**Table S1**). Nitrogen fluxes to the three litter pools from each of the three fine root pools are determined using the same fractions as used for carbon fluxes and their C/N ratios.

Additionally, maintenance and growth respiration follow the current ELM implementation (Oleson et al. 2013). Maintenance respiration rate is related to temperature and tissue N content without further differentiating intrinsic respiration rate and temperature sensitivity among TAM roots; varying N content differentiates respiration among TAM roots. Growth respiration is still calculated as a factor of 0.3 (***grperc***) times the total carbon in new growth including the fine-root system.

2 Parameterization and Simulation

We implemented the changes as detailed above to realize the TAM structure in sELM. This implementation is referred to as TAM model (or TAM in short), while the original version is referred to as ELM. For an illustration purpose, we parameterized TAM and ELM for 2 temperate forests across the East US: Howland Forest (https://ameriflux.lbl.gov/sites/siteinfo/US-Ho1; Hollinger et al. 2021; a single temperate evergreen needleleaf PFT) and Ozark (https://ameriflux.lbl.gov/sites/siteinfo/US-MOz; a single temperate deciduous broadleaf PFT; Gu et al. 2016). We used FRED (v3.0), a global Fine-Root Ecology Database to address below-ground challenges in plant ecology (https://roots.ornl.gov/; Iversen et al. 2017; Iversen and McCormack 2021), FunFun, a fungal trait database (Zanne et al. 2020), and published literature to derive PFT-specific parameter values/ranges for TAM (**Table S1**). Simulation at each site was driven by forcings including daily radiation, maximum and minimum temperature, precipitation, day length, and a constant CO_2 level (cycled 6 times).

3 Uncertainty and Sensitivity Analysis

TAM was compared with ELM (with default parameterization) by accounting for structural and parameter uncertainties introduced by the novel 3-pool structure. These comparisons involved outputs of interest including fluxes of GPP and heterotrophic respiration and pools of leaf and fine-root system TAM, as well as the nitrogen limitation factors for plant growth (i.e., Fraction of Potential Growth, $FPG = F_{plant\_uptake}/F_{plant\_demand}$).

First, one conservative case of preserving the fine-root system C/N of ELM in TAM was examined to see impacts of this structural shift and its associated uncertainties. To preserve the fine-root system C/N in TAM (i.e., the default parameterization of C/N = 42), two specific scenarios were derived by solving the following equation, **Eq.7**, conditioned on the observed pattern of ascending C/N across the hierarchical branching orders within fine-root systems (e.g., McCormack et al. 2015a) and on prescribing one case of descending allocation from T through A (**TAM_descend**) and one case of ascending allocation (**TAM_ascend**):

$$\begin{cases} \sum_{i=1}^{3} \frac{frootcn\_i}{frootpar\_i} = 42 \\ frootcn\_t > frootcn\_a > frootcn\_m \\ frootpar\_i = [0.5,0.3,0.2] \; or \; [0.2,03,0.5] \end{cases} \quad (7)$$

By prescribing two alternatives of partitioning fraction vector, the equation has two corresponding closed solutions of ***frootcn_i*****:** [60,42,24] or [72,42,36]. In other words, by preserving the fine-root system C/N and keeping the same phenology and distribution between ELM and TAM, the uncertainty of the TAM structure for these two scenarios potentially arose from parameters of only chemistry and longevity. On top of these two cases, a structural uncertainty arising from nitrogen-

204 constrained dynamic vertical distribution of new allocation was also examined, which were
205 referred to as **TAM_descend_dd** and **TAM_ascend_dd**, respectively.

206 Next, without preserving the C/N ratio, a radical case with full implementation of TAM
207 (including phenology) was compared with ELM. This comparison, relative to the above case,
208 accounted for uncertainty arising from parameters including C/N and partitioning (6 parameters)
209 and phenology-related parameters [3 parameters: ***gdd_crit*** (for evergreen PFT only)**,**
210 ***gdd_crit_gap, fcur***] **(Table S1)**. That is, varying the partitioning and C/N parameters freely and
211 phenology-related parameters under a full implementation of the proposed implementation of
212 TAM, changes relative to ELM and their uncertainty were attributed to these newly introduced
213 parameters.

214 Finally, a global sensitivity analysis of TAM was performed with 8 (7 for evergreen PFT
215 which does not have ***crit_dayl***) more existing parameters in ELM (**Table S2**). All parameter
216 uncertainty was quantified by 1080 ensemble runs from Monte-Carlo sampling from parameters'
217 uniform uncertainty ranges and uncertainty propagation through the model. Attribution of TAM
218 uncertainty was then achieved via variance-based sensitivity analysis with Sobol's sensitivity
219 indices (Sobol 2003; Ricciuto et al. 2018). The Sobol's sensitivity indices were indirectly derived
220 from a polynomial chaos expansion of the outputs via a new Weighted Iterative Bayesian
221 Compressive Sensing (WIBCS) algorithm using the Uncertainty Quantification Toolkit (UQTk
222 v3.0.2; https://github.com/sandialabs/UQTk).

Table S1. **List of introduced parameters and their uncertainty ranges.**

Parameter	Description	Unit	Range(evergreen/deciduous)	Reference
frootcn_t	C/N of T root	-	[20,184]/[19, 116]	FRED v3
frootcn_a	C/N of A root	-	[11,119]/[9, 81]	FRED v3
frootcn_m	C/N of M root	-	[7,25]/[7, 25]	Zanne et al. 2019
frootpar_t	Fraction of total allocation to T	-	[0.05, 0.95]	
frootpar_a	Fraction to total allocation to A	-	[0.05, 0.95]	
frootpar_m	Fraction to total allocation to M	-	[0.05, 0.95]	
frootlong_t	Longevity of T	year	[3, 10]	Matamala et al. 2003; Xia et al. 2010
frootlong_a	Longevity of A	year	[0.5, 4]	Matamala et al. 2003; Xia et al. 2010
frootlong_m	Longevity of M	year	[0.13, 1]	Pepe et al. 2018
fr_flab_t	Fraction of labile carbon in T	-	[0.125, 0.375]	± 50% of default value
fr_flab_a	Fraction of labile carbon in A	-	[0.125, 0.375]	± 50% of default value
fr_flab_m	Fraction of labile carbon in M	-	[0.125, 0.375]	± 50% of default value
fr_flig_t	Fraction of lignin carbon in T	-	[0.125, 0.375]	± 50% of default value
fr_flig_a	Fraction of lignin carbon in A	-	[0.125, 0.375]	± 50% of default value
fr_flig_m	Fraction of lignin carbon in M	-	[0.125, 0.375]	± 50% of default value
fr_fcel_t	Fraction of cellulose/hemicellulose C in T	-	[0.25, 0.75]	± 50% of default value
fr_fcel_a	Fraction of cellulose/hemicellulose C in A	-	[0.25, 0.75]	± 50% of default value
fr_fcel_m	Fraction of cellulose/hemicellulose C in M	-	[0.25, 0.75]	± 50% of default value
mort_depth_efolding	Rate of mortality decrease with depth	-	[187.15e-3,935.75e-3]	Iversen et al. 2008; McCormack et al. 2012; Germon et al 2015; Gu et al. 2017
gdd_crit_gap	Difference in GDD between root and leaf onset	℃ *day	[-300, 300]	Expert judgement

Table S2. List of existing parameters of interest in ELM and their uncertainty ranges.

Parameter	Description	Unit	Range(evergreen/deciduous)
gdd_crit	Leaf onset GDD	°C *day	150, 750
fcur	fraction of root allocation to display in current time step	-	[0.5, 1.0]/[0, 1]
froot_leaf	ratio of new fine root to new leaf carbon allocation	-	[0.5, 1.5]
slatop	Specific leaf area at canopy top	$m^2\ gC^{-1}$	[0.005,0.015]/[0.015,0.045]
crit_dayl	Critical day length for leaf senescence in deciduous	Seconds	[36000, 43000]
leafcn	leaf C/N	-	[17.5, 52.5]/[12.5, 37.5]
roota_par	Rooting depth distribution parameter	m^{-1}	[1.5,4.5]/[3, 9]
rootb_par	Rooting depth distribution parameter	m^{-1}	[0.625, 1.875]/[1, 3]
br_mr	Base rate for maintenance respiration (MR)	umol $m^{-2}\ s^{-1}$	[1.26e-06, 3.78e-06]
q10_mr	Temperature sensitivity for MR	-	[0.75, 2.25]

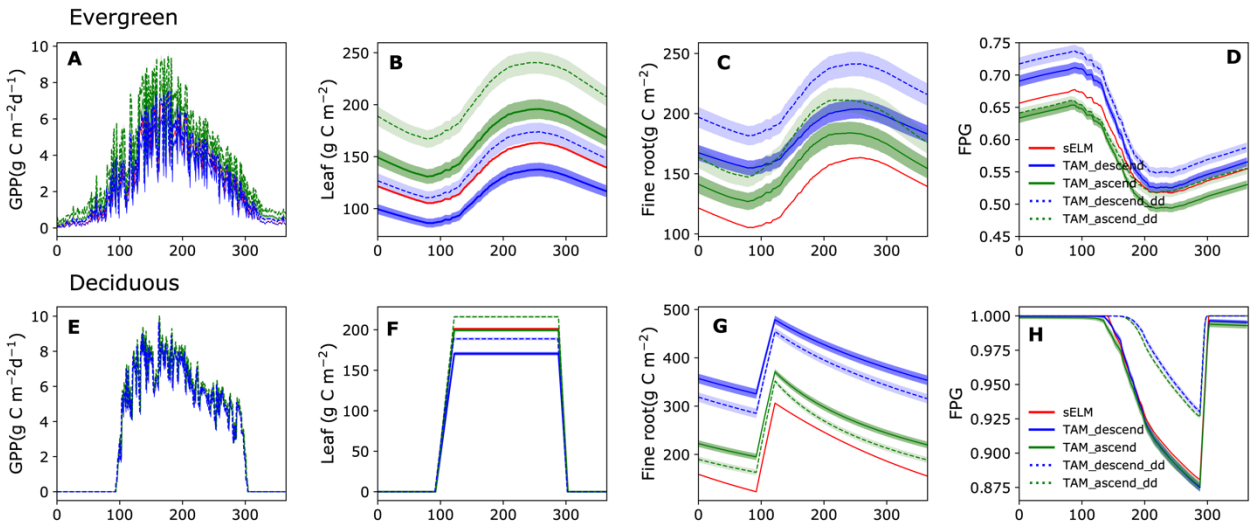

Fig. S1 Annual cycle of GPP, leaf mass, and fine-root system mass, as well as FPG (Fraction of Potential Growth) of TAM against the 1-pool structure of ELM (i.e., sELM) under preservation of fine-root system stoichiometry.

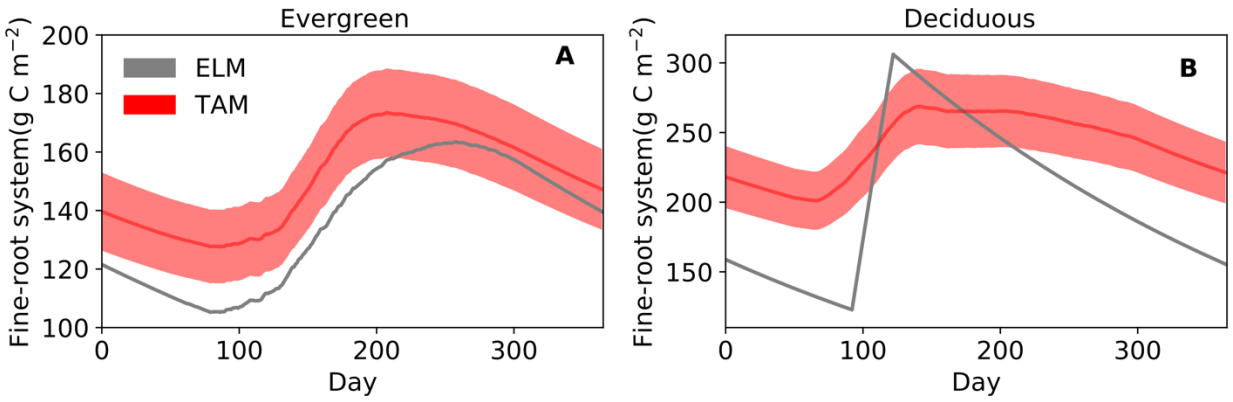

241

242 **Fig. S2 Seasonal variation in fine-root system biomass of radical TAM corresponding to Fig.4**

243 **in the main text**.

244

245

246

247

248

249

250

251

252

253

254

255

256

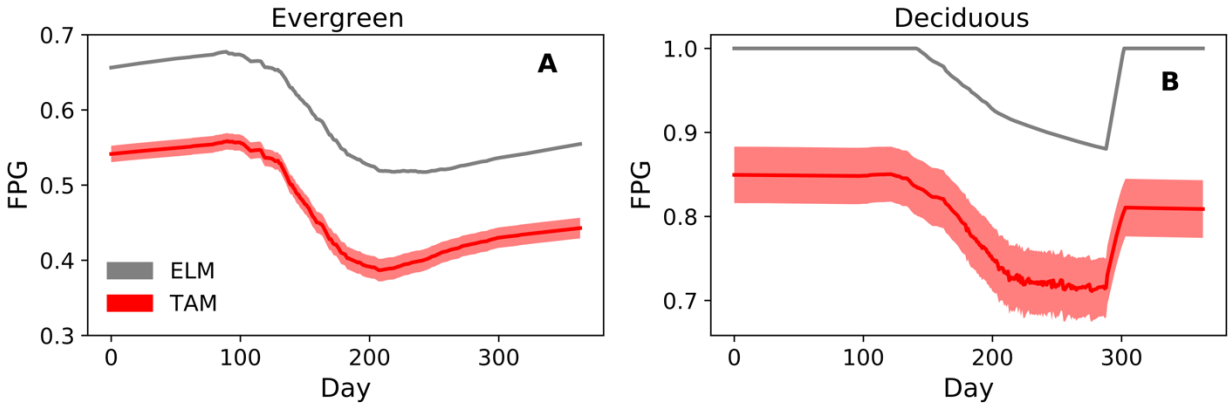

Fig. S3 Seasonal variation in FPG (Fraction of Potential Growth) under a full implementation of TAM corresponding to Fig.4 in the main text.

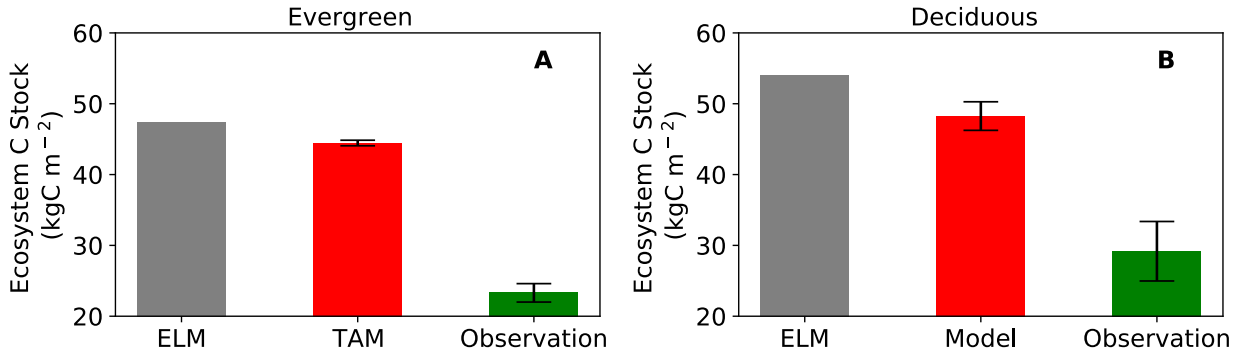

Fig. S4 Radical TAM brings simulated total ecosystem carbon stocks closer to observations. Observation in the evergreen forest is based on Hollinger et al. (2021), while the observation in the deciduous forest per Chen et al. (2015). Error bars represent 95% confidence intervals.

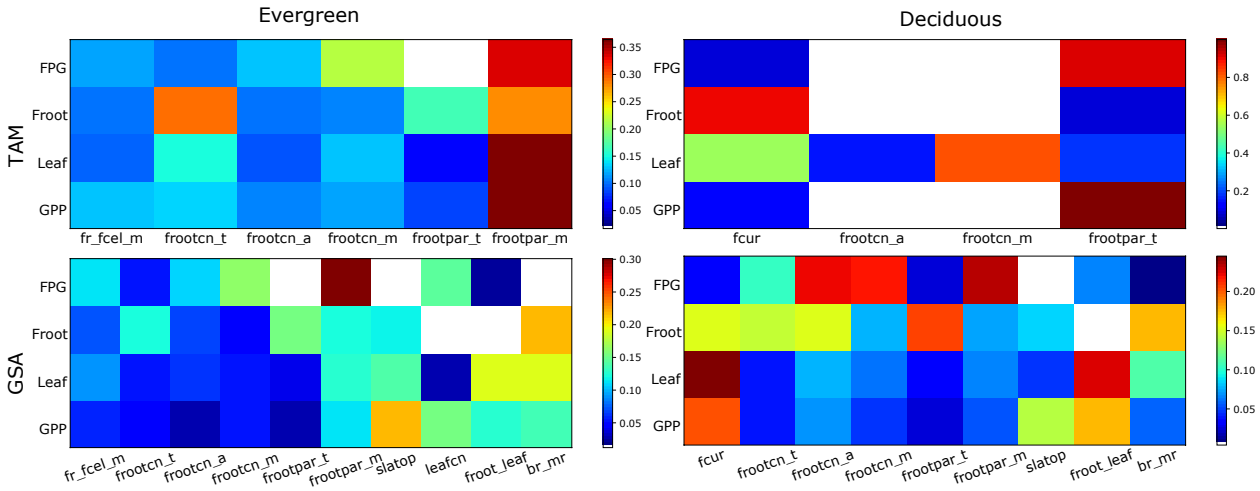

292

293 **Fig. S5 Attribution of TAM and global uncertainty with the main effect sensitivity index for**

294 **the two sites**. The TAM sensitivity corresponds to the conservative case of **Fig. 3** in the main text.

295 The Global Sensitivity Analysis (GSA) also includes some of existing parameters (**Table S2**).

296 Only the most relevant input parameters for each forest site are shown. The color code for each

297 row is scaled according to the highest contributor to improve visibility.

298

299 **References**

300 Abramoff, R. Z., & Finzi, A. C. (2015). Are above-and below-ground phenology in sync? New

301 Phytologist, 205, 1054-1061.

302

303 Allen, M. F., & Kitajima, K. (2013). In situ high-frequency observations of mycorrhizas. New

304 Phytologist, 200, 222-228.

305

306 Baddeley, J. A., & Watson, C. A. (2005). Influences of root diameter, tree age, soil depth and

307 season on fine root survivorship in *Prunus avium*. Plant and Soil, 276, 15-22.

308

309 Burrows, S. M., Maltrud, M., Yang, X., Zhu, Q., Jeffery, N., Shi, X., ... & Leung, L. R. (2020).
310 The DOE E3SM v1.1 biogeochemistry configuration: Description and simulated ecosystem-
311 climate responses to historical changes in forcing. Journal of Advances in Modeling Earth
312 Systems, 12, e2019MS001766.
313
314 Chen, J., Xu, J., Jensen, R., & Kabrick, J. (2015). Changes in aboveground biomass following
315 alternative harvesting in oak-hickory forests in the eastern USA. iForest-Biogeosciences and
316 Forestry, 8, 652.
317
318 Edwards, E. J., Benham, D. G., Marland, L. A., & Fitter, A. H. (2004). Root production is
319 determined by radiation flux in a temperate grassland community. Global Change Biology 10,
320 209-227.
321
322 Eissenstat, D. M., & Yanai, R. D. (1997). The ecology of root lifespan. Advances in Ecological
323 Research 27, 1-60.
324
325 Espeleta, J. F., West, J. B., & Donovan, L. A. (2009). Tree species fine-root demography parallels
326 habitat specialization across a sandhill soil resource gradient. Ecology 90, 1773-1787.
327
328 Germon, A., Cardinael, R., Prieto, I. et al. (2016). Unexpected phenology and lifespan of shallow
329 and deep fine roots of walnut trees grown in a silvoarable Mediterranean agroforestry system. Plant
330 Soil 401, 409–426.
331

Golaz, J.-C., Caldwell, P. M., Van Roekel, L. P., Petersen, M. R., Tang, Q., Wolfe, J. D., et al. (2019). The DOE E3SM coupled model version 1: Overview and evaluation at standard resolution. Journal of Advances in Modeling Earth Systems, 11, 2089–2129.

Gu, L., Pallardy, S. G., Yang, B., Hosman, K. P., Mao, J., Ricciuto, D., ... & Sun, Y. (2016). Testing a land model in ecosystem functional space via a comparison of observed and modeled ecosystem flux responses to precipitation regimes and associated stresses in a Central US Forest. Journal of Geophysical Research: Biogeosciences 121, 1884-1902.

Gu, J., Wang, Y., Fahey, T.J. et al. (2017). Effects of root diameter, branch order, soil depth and season of birth on fine root life span in five temperate tree species. European Journal of Forest Research 136, 727-738.

Hendrick, R. L., & Pregitzer, K. S. (1993). Patterns of fine root mortality in two sugar maple forests. Nature 361, 59-61.

Hendrick, R. L., & Pregitzer, K. S. (1997). The relationship between fine root demography and the soil environment in northern hardwood forests. Ecoscience, 4, 99-105.

Hollinger, D. Y., Davidson, E. A., Fraver, S., Hughes, H., Lee, J. T., Richardson, A. D., ... & Teets, A. Multi-Decadal Carbon Cycle Measurements Indicate Resistance to External Drivers of Change at the Howland Forest AmeriFlux Site. Journal of Geophysical Research: Biogeosciences e2021JG006276.

Huang, J., Hammerbacher, A., Gershenzon, J., van Dam, N. M., Sala, A., McDowell, N. G., ... & Hartmann, H. (2021). Storage of carbon reserves in spruce trees is prioritized over growth in the face of carbon limitation. Proceedings of the National Academy of Sciences 118, e2023297118

Iversen, C. M., Ledford, J., & Norby, R. J. (2008). CO_2 enrichment increases carbon and nitrogen input from fine roots in a deciduous forest. New Phytologist, 179, 837-847.

Iversen, C. M. et al. (2017). A global Fine-Root Ecology Database to address below-ground challenges in plant ecology. New Phytologist, 215, 15–26.

Joslin, J. D., Gaudinski, J. B., Torn, M. S., Riley, W. J., & Hanson, P. J. (2006). Fine-root turnover patterns and their relationship to root diameter and soil depth in a ^{14}C-labeled hardwood forest. New Phytologist, 172, 523-535.

Levine, E. R., Knox, R. G., & Lawrence, W. T. (1994). Relationships between soil properties and vegetation at the Northern Experimental Forest, Howland, Maine. Remote Sensing of Environment 47, 231-241.

Lu, D. and Ricciuto, D. (2019) Efficient surrogate modeling methods for large-scale Earth system models based on machine-learning techniques. Geoscientific Model Development 12, 1791-1807

McCormack, M. L., Pritchard, S. G., Breland, S., Davis, M. A., Prior, S. A., Brett Runion, G., ... & Rogers, H. H. (2010). Soil fungi respond more strongly than fine roots to elevated CO_2 in a model regenerating longleaf pine-wiregrass ecosystem. Ecosystems, 13, 901-916.

McCormack, M.L., Adams, T. S., Smithwick, E. A., & Eissenstat, D. M. (2012). Predicting fine root lifespan from plant functional traits in temperate trees. New Phytologist 195, 823-831.

McCormack, M. L., I. A. Dickie, D. M. Eissenstat, T. J. Fahey, C. W. Fernandez, D. Guo, H.-S. Helmisaari, E. A. Hobbie, C. M. Iversen, R. B. Jackson, J. Leppälammi-Kujansuu, R. J. Norby, R. P. Phillips, K. S. Pregitzer, S. G. Pritchard, B. Rewald, M. Zadworny (2015a). Redefining fine roots improves understanding of below-ground contributions to terrestrial biosphere processes. New Phytologist. 207, 505–518.

McCormack, M. L., Gaines, K. P., Pastore, M., & Eissenstat, D. M. (2015b). Early season root production in relation to leaf production among six diverse temperate tree species. Plant and Soil, 389, 121-129.

Oleson, K., Lawrence, D., Bonan, G., Drewniak, B., Huang, M., Koven, C., ... & Yang, Z. (2013). Technical description of version 4.5 of the Community Land Model (CLM), NCAR. National Center for Atmospheric Research (NCAR) Boulder, Colorado.

Perry, T. O. (1971). Dormancy of Trees in Winter: Photoperiod is only one of the variables which interact to control leaf fall and other dormancy phenomena. Science, 171, 29-36.

Pregitzer, K. S., Kubiske, M. E., Yu, C. K., & Hendrick, R. L. (1997). Relationships among root branch order, carbon, and nitrogen in four temperate species. Oecologia, 111, 302-308.

Pregitzer, K. S., Hendrick, R. L., & Fogel, R. (1993). The demography of fine roots in response to patches of water and nitrogen. New Phytologist, 125, 575-580.

Radville, L., McCormack, M. L., Post, E., & Eissenstat, D. M. (2016). Root phenology in a changing climate. Journal of Experimental Botany, 67, 3617-3628.

Reid, J. B., Sorensen, I., & Petrie, R. A. (1993). Root demography in kiwifruit (*Actinidia deliciosa*). Plant, Cell & Environment, 16, 949-957.

Ricciuto, D., Sargsyan, K., & Thornton, P. (2018). The impact of parametric uncertainties on biogeochemistry in the E3SM land model. Journal of Advances in Modeling Earth Systems, 10, 297–319.

Riley, W. J., Gaudinski, J. B., Torn, M. S., Joslin, J. D., & Hanson, P. J. (2009). Fine-root mortality rates in a temperate forest: estimates using radiocarbon data and numerical modeling. New Phytologist, 184, 387-398.

Sobol, I. M. (2003). Theorems and examples on high dimensional model representation. Reliability Engineering and System Safety, 79, 187–193.

Steinaker DF, Wilson SD. 2008. Phenology of fine roots and leaves in forest and grassland. Journal of Ecology, 96, 1222–1229.

Steinaker DF, Wilson SD, Peltzer DA. 2010. Asynchronicity in root and shoot phenology in grasses and woody plants. Global Change Biology 16, 2241–2251.

Tierney, G. L., & Fahey, T. J. (2002). Fine root turnover in a northern hardwood forest: a direct comparison of the radiocarbon and minirhizotron methods. Canadian Journal of Forest Research, 32, 1692-1697.

Xia, M., Guo, D., & Pregitzer, K. S. (2010). Ephemeral root modules in *Fraxinus mandshurica*. New Phytologist, 188, 1065-1074.

Zanne, A. E., Abarenkov, K., Afkhami, M. E., Aguilar-Trigueros, C. A., Bates, S., Bhatnagar, J. M., ... & Treseder, K. K. (2020). Fungal functional ecology: bringing a trait-based approach to plant-associated fungi. Biological Reviews 95, 409-433.